JACS
JOURNAL OF THE AMERICAN CHEMICAL SOCIETY
Article
pubs.acs.org/JACS

Steering On-Surface Polymerization with Metal-Directed Template

Tao Lin,[†] Xue Song Shang,[‡] Jinne Adisoejoso,[†] Pei Nian Liu,*[,‡] and Nian Lin*[,†]

[†]Department of Physics, The Hong Kong University of Science and Technology, Clear Water Bay, Hong Kong, China

[‡]Shanghai Key Laboratory of Functional Materials Chemistry and Institute of Fine Chemicals, East China University of Science and Technology, Meilong Road 130, Shanghai, China

Supporting Information

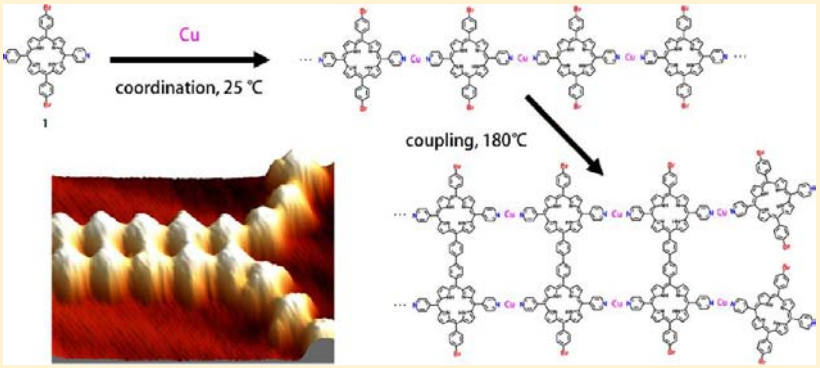

ABSTRACT: On-surface polymerization represents a novel bottom-up approach for producing macromolecular structures. To date, however, most of the structures formed using this method exhibit a broad size distribution and are disorderly adsorbed on the surface. Here we demonstrate a strategy of using metal-directed template to control the on-surface polymerization process. We chose a bifunctional compound which contains pyridyl and bromine end groups as the precursor. Linear template afforded by pyridyl−Cu−pyridyl coordination effectively promoted Ullmann coupling of the monomers on a Au(111) surface. Taking advantage of efficient topochemical enhancement owing to the conformation flexibility of the Cu−pyridyl bonds, macromolecular porphyrin structures that exhibit a narrow size distribution were synthesized. We used scanning tunneling microscopy and kinetic Monte Carlo simulation to gain insights into the metal-directed polymerization at the single molecule level. The results reveal that the polymerization process profited from the rich chemistry of Cu which catalyzed the C−C bond formation, controlled the size of the macromolecular products, and organized the macromolecules in a highly ordered manner on the surface.

INTRODUCTION

On-surface polymerization refers to the process in which molecular precursors are covalently linked on a surface. It represents a new strategy to synthesize macromolecular systems. The earlier successful attempts were demonstrated at liquid−solid interfaces.[1−5] In 2007, Grill et al. demonstrated that dimeric, polymeric, and network structures can be formed on a Au(111) surface under ultrahigh-vacuum conditions through covalent coupling of bromine-terminated porphyrin precursors.[6] In less than six years, on-surface coupling based on various reaction routes has generated a large variety of macromolecular systems, including polymeric chains,[7−12] hyper-branched oligomers,[13,14] graphene ribbons,[15] porous molecular networks,[16−24] super honeycomb frameworks,[25] etc.[26−31] This progress has attracted increasing attention, and the field of on-surface polymerization is growing quickly.[32−34]

The nonreversibility of the covalent bonds, however, introduces kinetic trapping in the polymerization processes. As a result, the size of the macromolecular systems formed by on-surface polymerization cannot be controlled accurately, and the products are randomly distributed on surface. To overcome this obstacle, various strategies have been proposed.[12,22−24,26,31] Linderoth et al. reported that organizational motifs in preassembled structures formed from one of the reactants may be retained in the final product structure.[26] Lackinger et al. showed that polycondensation (dehydration) of boronic acid in the presence of water led to covalent networks of high structural quality.[22,23] Chi et al. used troughs on the gold surface to line up the polymer chains formed out of alkane monomers.[12] More recently, Grill et al. used I- and Br-functionalized precursors to control the outcome structures via stepwise coupling.[31] Here we developed an effective approach of using metal−ligand coordination as template to steer the on-surface polymerization process. The resulting macromolecular structures exhibit a very narrow size distribution and are organized hierarchically through supramolecular assembly.

Template synthesis is an area where "molecular and supramolecular science meet".[35,36] It uses noncovalent binding motifs to steer the formation of covalently linked products.

Received: December 5, 2012
Published: February 21, 2013

   dx.doi.org/10.1021/ja311890n | J. Am. Chem. Soc. 2013, 135, 3576−3582

This approach dates back to the 1960s when Busch studied and classified different modes of templates.[37] Metal−ligand binding, hydrogen bonding, and $\pi-\pi$ interactions have been used as templates to control the synthesis of molecules with remarkable structural characteristics that are otherwise difficult to achieve.[36] An elegant example of metal-directed template was demonstrated by Anderson and his co-workers: belt-like nanorings consisting of 6, 8, 12, or more porphyrin units were prepared using radial oligo-pyridine templates.[38] Another type of template is linear template which promotes metal-assisted or metal-catalyzed solid-state dimerization within a 1D coordination polymer.[39] This type of template has the potential to self-replicate, since the product can in principle be identical to the template, akin to the replication of DNA.[40] In this study, we used linear template to control the on-surface polymerization.

METHODS

Experiments were performed in an ultrahigh-vacuum system (Omicron Nanotechnology) with base pressure below 5×10^{-10} mbar. A single-crystalline Au(111) substrate was prepared by argon ion sputtering and annealing at ∼630 °C, resulting in terraces of ∼100 nm wide. Copper atoms were deposited by an electron-beam evaporator on the substrate which was held at room temperature (23 °C). The copper deposition rate was determined through analyzing the area of Cu islands formed on a clean Au substrate. The crucibles containing the molecules were then heated in an organic molecular beam deposition source (Dodecon) to a certain evaporating temperature (350, 320, 370, and 320 °C for compounds **1**−**4** in Scheme 1, respectively), and the molecules were deposited on the substrate held at room temperature or higher. Scanning tunneling microscopy (STM) measurements were performed at 23 °C if not indicated otherwise in a constant-current mode at 1.0−1.4 V positive or negative bias and 0.2−0.4 nA tunneling current. The STM scanning scales were calibrated using Au(111) as a standard sample.

Scheme 1. Porphyrin Compounds Used in This Study

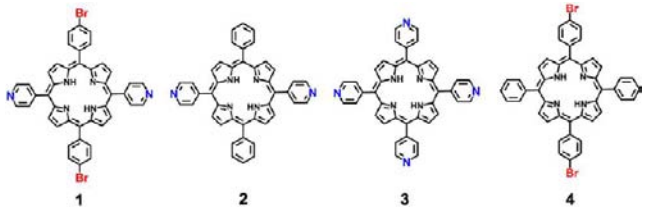

The kinetic Monte Carlo (KMC) simulations were performed on a 100×100 square lattice, which corresponds to one monolayer of a molecule network containing 33×33 molecules. Periodic boundary conditions were applied. The molecules were deposited randomly onto the substrate lattice. Desorption of the molecules from the substrate was not allowed. The molecules could hop to the nearest-neighboring site or rotate by 90° clockwise or anticlockwise. When one molecule attached to another molecule in a configuration in which pyridyl (py) functions of the two molecules were aligned head to head (py−py), a coordination bond was formed. And when one molecule encountered another in a Br−Br configuration, the rate at which a covalent bond was formed was determined by an energy barrier of 1.2 eV. The details of the KMC simulation algorithm can be found in ref. 41 and in the Supporting Information (SI).

RESULTS AND DISCUSSION

Identification and Verification of On-Surface Polymerization. Compound **1** (Scheme 1) provides py groups as coordination sites for metal-directed template and bromine groups as the Ullmann coupling sites. We found that in the presence of Cu, the monomers of **1** assembled with Cu atoms forming one-dimensional metallosupramolecular single-row (SR) chains at 23 °C (Figure 1a). Since the SR chains emerged only upon codeposition of Cu and **1** and the nearest-neighboring molecule distance (1.9 nm) is the same as the length of the coordination chains formed by **2** and Cu (Figure S1), we conclude that the SR chains were stabilized by 2-fold py−Cu−py coordination.[41,42] The py groups at the *trans*-positions of **1** give rise to the linear morphology of the model shown in Figure 1a. The coordinated Cu atoms were not resolved in the STM data, presumably due to electronic effects or tip conditions. It is worth noting that many of the SR chains exhibited a bent or curved shape, implying a high degree of flexibility of the py−Cu−py coordination. This bond angle flexibility even allowed a large section of chains to shift on the surface without fragmentation (cf. Figure 3c,e and Figure S1). The bond angle flexibility is associated with the two-fold configuration of the py−Cu−py coordination which is known to exhibit a high degree of conformational flexibility.[43]

After annealing at 180 °C for 30 min, ladder-shaped chains consisting of double or triple rows (DR or TR, respectively) of monomers appeared, as shown in Figure 1b. Figure 1c is a high resolution STM image of a DR chain. Detailed inspection reveals that there is a gap between the neighboring molecules along the chain direction (cf. the blue line in Figure 1c), whereas the two molecules perpendicular to the chain direction are linked by a bridge (cf. the red line in Figure 1c). The separation between neighboring molecules (center-to-center) perpendicular to the chain direction is 1.73 nm, which is shorter than the separation between neighboring molecules (center-to-center) along the chain direction (1.95 nm) but the same as the intermolecular distance in the covalently linked porphyrin macromolecules.[6] These structural characteristics clearly indicate that the monomers that are 1.73 nm apart are covalently bonded dimeric macromolecules and that these macromolecules are linked by py−Cu−py coordination along the chain direction, forming the DR chains as illustrated by the model in Figure 1b. Another piece of evidence of the proposed structure is the protrusions at the sides of the porphyrin dimers, as marked by the arrow in Figure 1c. These protrusions, which have been observed before and identified as bromine atoms,[6,31] indicate that the Br groups are positioned at right angles to the DR chain direction. To further verify the proposed DR model, we added a batch of compound **3** molecules to a sample which was already covered with the DR chains in advance. We found that the compound **3** molecules did not attach to the sides of DR chains but rather formed 2D coordination islands that attached to the end of the pre-existing DR chains (Figure S2). It is thus evident that the py groups are positioned along the chain direction.

Cu-Catalyzed Ullmann Coupling. Apparently, 180 °C annealing activated the C−C coupling reaction of **1**, leading to the formation of the covalently bonded porphyrin dimers.[6,8,11,15,17,25,31,44] The reaction temperature is lower than that of the same coupling reaction which is thermally activated on a Au(111) surface,[6,31,44] hinting that Cu acts as a catalyst. Although the reaction steps were not accessible using STM, we identified the intermediate Cu organometallic state in the samples annealed at 120 °C (Figure S3), which evidenced that Cu atoms were involved in the coupling reactions.[45] To quantitatively examine the effect of Cu, we varied the Cu dosage and annealing parameters. First, in a control experiment, we prepared a sample deposited with **1** but without Cu. We found that in the absence of Cu, the ratio of C−C bond

dx.doi.org/10.1021/ja311890n | J. Am. Chem. Soc. 2013, 135, 3576−3582

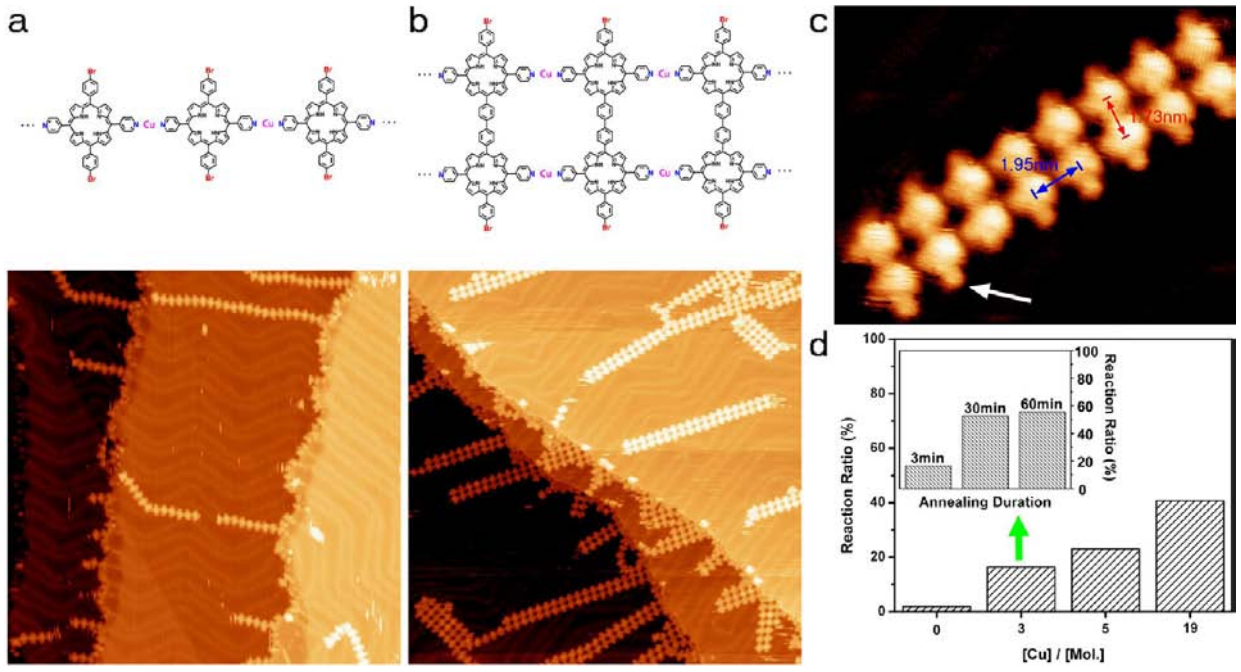

Figure 1. Structures formed from **1** and Cu on a Au(111) surface. STM topographs (100 ×100 nm) showing (a) SR coordination chains formed at 25 °C and (b) DR and TR chains formed after 180 °C annealing. (c) High-resolution STM topograph of a DR chain. The arrow is pointing at Br. (d) Reaction ratios at different Cu dosages. Inset shows the reaction ratios at a fixed Cu dosage but with different annealing durations.

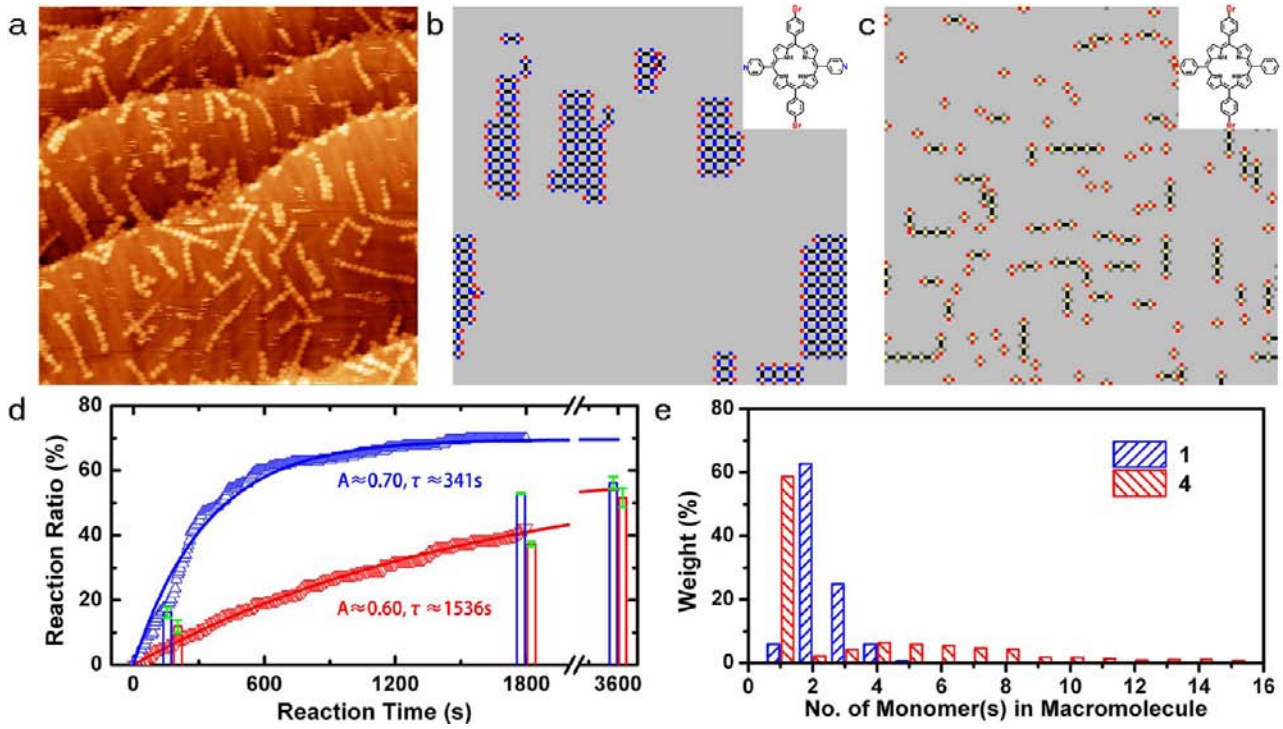

Figure 2. Comparison of the polymerization of **1** and **4**. (a) STM topograph (100 ×100 nm) showing macromolecular structures formed from **4** (data acquired at 200 K). (b,c) KMC simulated structures formed out of **1** and **4** (at 450K for 30 min). (d) Reaction ratios of **1** and **4** as a function of reaction time. Triangles represent simulated results, solid lines represent exponential fitting, and vertical bars represent experimental values. Blue (red) indicates **1**(**4**). (e) Experimental weight distribution of the macromolecular structures formed from **1** and **4** as a function of macromolecule size.

formation of **1** was <1.5% after annealing at 180 °C for 10 min. Figure 1d shows that under the same annealing temperature but for a shorter duration (180 °C for 3 min), adding Cu at a dosage of [Cu]/[Mol.] = 3 ([Cu] and [Mol.] refer to the surface coverage of deposited Cu atoms and that of deposited molecules of **1**, respectively) amplified the reaction ratio (reaction ratio is defined as the percentage of Br groups that were replaced by C−C bonds) by more than 10 times. When the Cu dosage was raised to [Cu]/[Mol.] = 5 and 19, the reaction ratios were amplified by 20 or 30 times, respectively.

dx.doi.org/10.1021/ja311890n | J. Am. Chem. Soc. 2013, 135, 3576−3582

These trials clearly demonstrated that Cu effectively promoted the coupling reaction, a process that can be considered as an Ullmann reaction occurring on the surface. Note that in the solution-phase reactions, the catalyst loading of the metal, such as Cu, is usually much smaller than that of the reactant. We attribute the high catalyst loading in this study to the immobilization of the reactant as coordinated chains and the reduced mobility of the Cu catalyst on the surface compared with the free movement and collision of the catalyst and the reactant in the solution phase. The inset in Figure 1d shows that at a constant Cu dosage, extending the annealing duration to 30 (60) min caused the reaction ratio to go up to 53% (56%). So at this Cu dosage, the reaction at 180 °C for 3 min was kinetic controlled. Interestingly, the reaction ratio after 60 min of annealing was not enhanced significantly as compared with that after 30 min of annealing. This finding implies that the coupling reaction was in a deep kinetic trap. It is worth noting that the reaction ratio did not reach 100% but was saturated at about 60% even with high Cu dosage and long annealing duration. This effect will be discussed in detail later.

Metal-Directed Template Afforded by py−Cu−py Coordination. To unravel the role of py functions, we compared the polymerization behavior of **1** and **4**. Figure 2a is a representative STM image of a sample deposited with **4** and Cu and annealed at 180 °C for 60 min. The figure shows covalently bonded polymeric chains.[6] (STM images of the sample annealed for other durations are shown in Figure S5.) We quantitatively compared the reaction ratios of **1** and **4** under the same Cu dosage and annealing treatment and found that the reaction ratios of **4** were always lower than those of **1**: 11% vs 16%, 38% vs 53%, and 51% vs 57% for 3, 30, and 60 min of annealing, respectively (represented by the vertical bars in Figure 2d). We used the KMC method to simulate the reactions of **1** and **4**. Figure 2b,c shows the simulated polymerization of **1** and **4** at 450K for 30 min, respectively. One can see that the molecules of **1** form ladder-like structures in which the monomers are linked by py−Cu−py coordination bonds (marked in blue), while in the orthogonal direction the monomers are coupled by covalent bonds (marked in black). Note that Figure 2b shows only one monomer not involved in the coupling reaction. In contrast, an appreciable amount (60%) of monomers of **4** is still present in Figure 2c. The simulated reaction ratios of the two compounds as a function of annealing time are plotted in Figure 2d. Each set of data can be fitted using the function $A(1 - e^{-t/\tau})$. The time constant τ characterizes the reaction rate. The time constant of **1** (341 s) is about one-fifth of that of **4** (1536 s). The prefactor A, however, is comparable for **1** and **4**. Thus the simulation reveals that the py−Cu−py coordination significantly enhanced the coupling reaction rates but did not change the reaction equilibrium. As shown in Figure 3d, the reaction ratios of **4** obtained experimentally are in good agreement with the simulated ones. The simulation of **1** reproduced qualitatively the trend of the experimental reaction ratios. However, the actual experimental values were lower than the simulated ones. This discrepancy might be associated with the fact that the parameters used in the simulation did not fully agree with the experimental ones. For example, surface steps and Cu density were excluded in the simulation.

We conducted statistical analysis of the experimental weight distribution of the macromolecular structures formed out of **1** or **4** after 60 min of annealing at 180 °C. The weight of macromolecules containing a specific number of monomers is defined as the percentage of monomers that form macromolecules of this size out of the total amount of monomers. Figure 2e shows that the weight distributions of two compounds exhibit distinctive characteristics. First, monomers account for 5% in **1** but almost 60% in **4**, which reflects the lower reaction rates of **4**. Second, the macromolecular structures formed from **4** exhibit a wide size distribution. For instance, structures as long as 15-mers can be found. In contrast, under the same experimental conditions, the macromolecular structures formed from **1** show a narrower size distribution in which the dimeric macromolecules are dominantly formed (63%) and the largest structure is the pentamer. Last but not least, the macromolecules formed out of **1** are regularly organized as chains on the surface through metal coordination, whereas the products of **4** are randomly distributed.

The reactions, which occurred at 180 °C or higher, could not be directly monitored using STM. Here we discuss two possible reaction mechanisms. One scenario is that the metal-coordinated SR chains decomposed upon annealing and some molecules formed covalent dimers, trimers or larger multimers. The coordination chains were formed when the sample was cooled. However, this process would generate macromolecules of a broad size distribution like that of compound **4**, since the py function would not play any role in such a process. Furthermore, the macromolecules of different sizes would be linked though metal coordination in the cooling process, which would result in chains consisting of sections of various width. In other words, the formed chains would not exhibit homogeneous width. But neither of these features was observed in the experiments, so we rule out this mechanism. The second mechanism is based on template-assisted coupling reaction, as illustrated in Scheme 2, where a DR chain is developed from a dimeric molecule seed step by step. The decomposition of the DR chain requires breaking two metal−ligand bonds simultaneously, which is very unfavorable energetically. Thus once formed, the DR chain does not decompose at the annealing temperature. At each growth step, an intermediate state is formed in which two precursor monomers are separately anchored through py−Cu−py coordination to the end dimer of the DR chain, as illustrated in the upper part of Scheme 2. In the intermediate state, the anchoring bonds of py−Cu−py coordination must be bent to avoid spatial conflict between the Br end groups of the two anchored molecules, as highlighted by the circle in Scheme 2. As discussed before, the bond angle of py−Cu−py coordination can deviate from 180°. This bond angle flexibility allows the intermediate state to be formed. The circles in Figure 3c mark several examples of the intermediate state. In the intermediate state, the Br groups of the two anchored molecules are brought into proximity (see the circled area in the upper part of Scheme 2). Such a configuration facilitates the Ullmann coupling reaction between the two Br ends as in topochemical polymerization processes.[46] As can be seen in the time sequence frames of the simulation (SI movie), most of the C−C bonds were formed between the neighboring monomers that were anchored to the existing chains though coordination bonds, so the reaction rate of the monomers in the intermediate state increased substantially in comparison with that of the reaction between the monomers that moved randomly on the surface. Hence we propose that Cu played a dual role in promoting the C−C bond formation. On the one hand, Cu reduced the reaction barrier as the catalyst in the

dx.doi.org/10.1021/ja311890n | J. Am. Chem. Soc. 2013, 135, 3576−3582

Scheme 2. Ullmann Coupling Assisted by the py−Cu−py Coordination Template Owing to Topochemical Enhancement

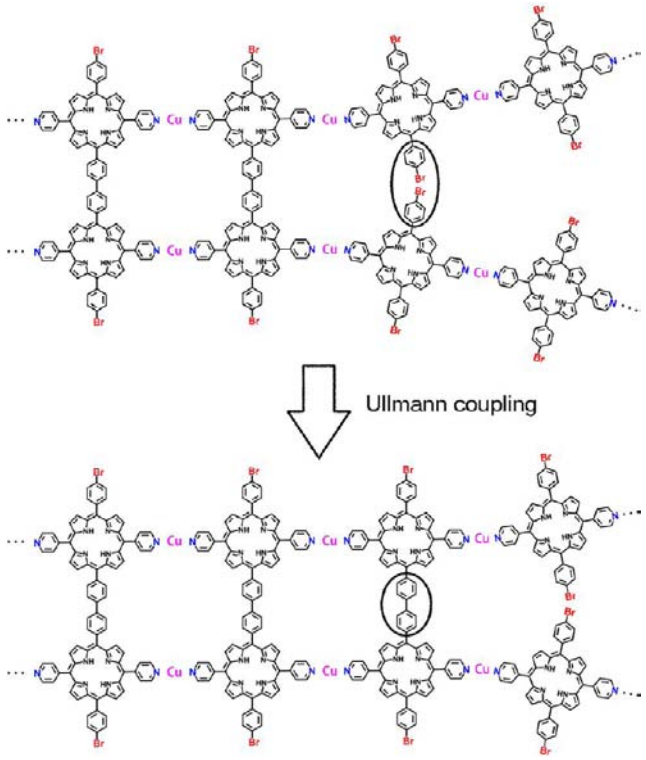

Ullmann reaction, and on the other hand, Cu ligated with py as template which further speeded up the reaction.

Size-Limited Polymerization. We now discuss the size distribution of the macromolecules. Figures 1b and 2d show that 180 °C annealing resulted in predominantly dimeric and trmeric structures. We annealed a series of samples deposited with **1** and Cu at different annealing temperatures (Figures S6 and S7). Figure 3a shows a representative STM image of a sample after annealing at 300 °C. One can see that most of the products are DR chains. Figure 3b shows the weight distribution of the macromolecular structures generated at different annealing temperatures. The weight of TR chains increases slightly at higher temperatures. Nevertheless, the high-temperature annealing did not significantly enhance the formation of larger oligomers. For example, in all cases, tetramers or larger are very rare, and the largest structure observed is heptamer structures, as marked by the arrow in Figure 3a. Above 180 °C, DR chains are always the most popular structure regardless of the annealing parameters (temperature and duration). The reaction ratios in all these trials are <60%. The saturation of the reaction ratio at 60% corroborates the predominant formation of DR chains (note that the reaction ratio is 50% when all monomers form dimeric macromolecules).

Besides the size limitation of the macromolecules, surprisingly, in all the samples, the chains have very smooth edges. This phenomenon reveals that: (1) attachment of individual monomers to the side of a chain is an unfavorable process and (2) in the case where a side attachment does occur, the attached monomers will quickly develop into a new row to the side of the chain. Both (1) and (2) can be understood by referring to the template effect discussed before. A precursor

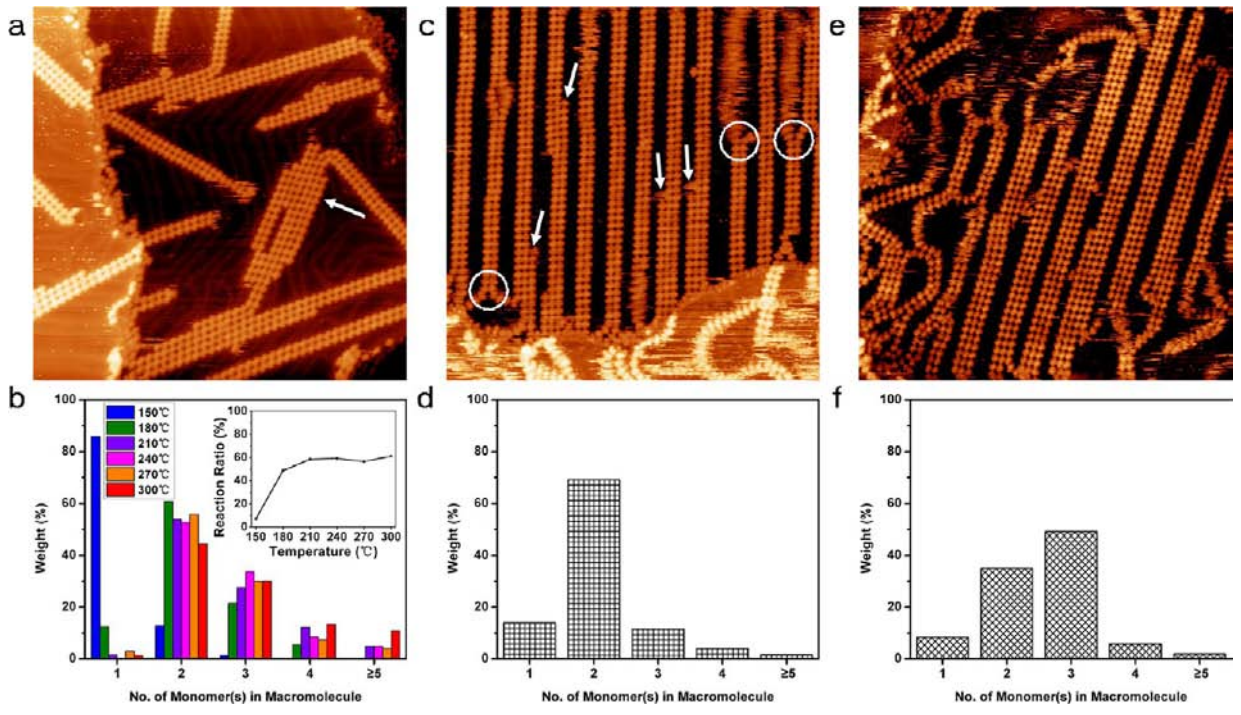

Figure 3. STM topographs (100 ×100 nm) and weight distributions of **1** with different preparation parameters. (a) Molecules were deposited on the substrate at room temperature and annealed at 300 °C. (b)Weight distribution of the macromolecular structures formed with different annealing treatments. Inset shows the corresponding reaction ratios. (c,d) The sample prepared in two steps, where in each step, molecules were deposited on the substrate at room temperature, annealed at 180 °C, and cooled down to room temperature. (e,f) Molecules were deposited at 240 °C on the substrate which was covered with Cu in advance.

dx.doi.org/10.1021/ja311890n | J. Am. Chem. Soc. 2013, 135, 3576−3582

monomer can attach to the side of a chain through a C−C bond, a process that requires overcoming an energy barrier. Being anchored to the ends of the existing chains through py−Cu−py coordination, however, is a process that does not require overcoming an energy barrier. So the precursor monomers prefer the latter process which then leads to the formation of dimeric structures and extend the chain's length, as illustrated in Scheme 2. In rare cases, precursor monomers might undergo covalent attachment to the side of DR chains. In such a situation, as illustrated in Scheme 3, the covalently attached monomer can anchor other monomer(s) through py−Cu−py coordination at its side(s). Owing to the topochemical enhancement effect discussed before, the anchored monomer(s) will form C−C bonds with the porphyrin unit(s) of the DR chain. Thus, the attachment of one monomer triggers the rapid growth of a new row which would become covalently bonded to the side of the existing DR chain. The simulated time sequence frames (SI movie) show the proposed process: Once a monomer is covalently attached to the side of a chain, a new row develops from it. To summarize, we found that the coordination template steered the polymerization process in such a way as to favor the replication of the existing smaller (dimeric and trimeric) structures over the growth of larger structures, which led to the predominant formation of the dimeric macromolecules.

Scheme 3. Growth of a New Row to the Side of a DR Chain Starting from an Initially-Attached Monomer Assisted by py−Cu−py Coordination Template

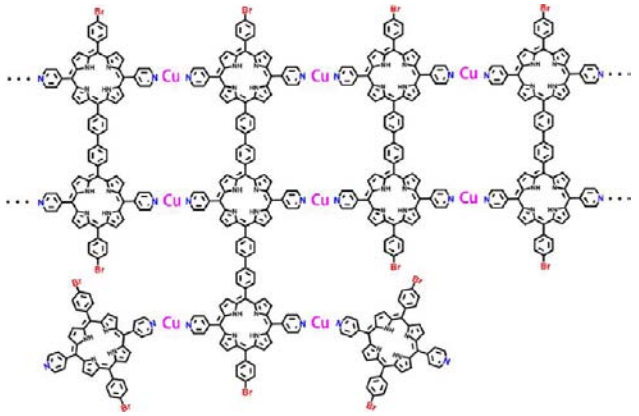

To test the proposed mechanism, we carried out the following control experiment: First we prepared a sample with DR chains of low surface coverage, then we deposited more molecules of **1** and Cu on the surface and annealed the sample at 180 °C for 30 min. One can see in Figure 3c that sections of several DR chains as marked by the arrows were widened and became TR chains. However, the STM (Figure 3c) and the weight distribution (Figure 3d) reveal that the DR chains are still the dominant structures. Thus it is obvious that the majority of the late-arriving molecules formed new DR chains or extended the pre-existing DR chains, which is consistent with the proposed mechanism. This reaction mechanism suggests that to enhance the yield of larger macromolecules, some larger macromolecular structures must be formed at the early stage of the reaction as seeds. These structures may trigger the formation of structures of the same size at the later stage of the reaction, i.e., a self-replicating process. We deposited molecules of **1** on a hot surface (240 °C) which was covered with Cu in advance. At a high reaction temperature, more covalently bonded trimers or other large macromolecules were generated. Figure 3e is a STM image of this sample. One can see that more TR chains were indeed formed. The weight distribution (Figure 3f) shows that the weight of the TR chains reached 50%, exceeding the weight of the DR chains.

CONCLUSION

In summary, the combined STM and KMC study of the specially designed bifunctional porphyrin compounds has provided insights into metal-directed template reactions on surfaces at the molecular level. The results reveal that the metal-directed template afforded by py−Cu−py coordination effectively alters the outcome structure of the on-surface polymerization. First, the dimeric structure is formed with a very high yield of >60% at 180 °C. Second, the macromolecules are organized by metal coordination into supramolecular chains on the surface. We believe these results will inspire the design and synthesis of size- and shape-controlled macromolecular systems in the fast emerging field of on-surface synthesis.

ASSOCIATED CONTENT

Supporting Information

Synthesis of compounds **1**−**4**, detailed KMC procedure and parameters, and supporting figures and movie. This material is available free of charge via the Internet at http://pubs.acs.org.

AUTHOR INFORMATION

Corresponding Author

phnlin@ust.hk; liupn@ecust.edu.cn

Notes

The authors declare no competing financial interest.

ACKNOWLEDGMENTS

This work was supported financially by the Hong Kong Research Grants Council (project no. 603611), the National Natural Science Foundation of China (project nos. 21172069 and 21190033), the Innovation Program of Shanghai Municipal Education Commission (project no. 12ZZ050), and the Fundamental Research Funds for the Central Universities.

REFERENCES

(1) Grim, P. C. M.; De Feyter, S.; Gesquière, A.; Vanoppen, P.; Rücker, M.; Valiyaveettil, S.; Moessner, G.; Müllen, K.; De Schryver, F. C. *Angew. Chem., Int. Ed.* **1997**, *36*, 2601.
(2) Okawa, Y.; Aono, M. *Nature* **2001**, *409*, 683.
(3) Okawa, Y.; Aono, M. *J. Chem. Phys.* **2001**, *115*, 2317.
(4) Sakaguchi, H.; Matsumura, H.; Gong, H.; Abouelwafa, A. M. *Science* **2005**, *310*, 1002.
(5) Sakaguchi, H.; Matsumura, H.; Gong, H. *Nat. Mater.* **2004**, *3*, 551.
(6) Grill, L.; Dyer, M.; Lafferentz, L.; Persson, M.; Peters, M. V.; Hecht, S. *Nat. Nanotechnol.* **2007**, *2*, 687.
(7) Matena, M.; Riehm, T.; Stöhr, M.; Jung, T. A.; Gade, L. H. *Angew. Chem., Int. Ed.* **2008**, *47*, 2414.
(8) Lipton-Duffin, J. A.; Ivasenko, O.; Perepichka, D. F.; Rosei, F. *Small* **2009**, *5*, 592.
(9) Schmitz, C. H.; Ikonomov, J.; Sokolowski, M. *J. Phys. Chem. C* **2009**, *113*, 11984.
(10) Jensen, S.; Früchtl, H.; Baddeley, C. J. *J. Am. Chem. Soc.* **2009**, *131*, 16706.

(11) Lipton-Duffin, J. A.; Miwa, J. A.; Kondratenko, M.; Cicoira, F.; Sumpter, B. G.; Meunier, V.; Perepichka, D. F.; Rosei, F. *Proc. Natl. Acad. Sci. U.S.A.* **2010**, *107*, 11200.
(12) Zhong, D.; Franke, J. -H.; Podiyanachari, S. K.; Blömker, T.; Zhang, H.; Kehr, G.; Erker, G.; Fuchs, H.; Chi, L. *Science* **2011**, *334*, 213.
(13) Weigelt, S.; Busse, C.; Bombis, C.; Knudsen, M. M.; Gothelf, K. V.; Lægsgaard, E.; Besenbacher, F.; Linderoth, T. R. *Angew. Chem., Int. Ed.* **2008**, *47*, 4406.
(14) Wang, S.; Wang, W.; Lin, N. *Phys. Rev. B.* **2012**, *86*, 045428.
(15) Cai, J.; Ruffieux, P.; Jaafar, R.; Bieri, M.; Braun, T.; Blankenburg, S.; Muoth, M.; Seitsonen, A. P.; Saleh, M.; Feng, X.; Müllen, K.; Fasel, R. *Nature* **2010**, *466*, 470.
(16) Zwaneveld, N. A. A.; Pawlak, R.; Abel, M.; Catalin, D.; Gigmes, D.; Bertin, D.; Porte, L. *J. Am. Chem. Soc.* **2008**, *130*, 6678.
(17) Gutzler, R.; Walch, H.; Eder, G.; Kloft, S.; Heckl, W. M.; Lackinger, M. *Chem. Commun.* **2009**, *29*, 4456.
(18) Tanoue, R.; Higuchi, R.; Enoki, N.; Miyasato, Y.; Uemura, S.; Kimizuka, N.; Stieg, A. Z.; Gimzewski, J. K.; Kunitake, M. *ACS Nano* **2011**, *5*, 3923.
(19) Schmitz, C. H.; Ikonomov, J.; Sokolowski, M. *J. Phys. Chem. C* **2011**, *115*, 7270.
(20) Schlögl, S.; Sirtl, T.; Eichhorn, J.; Heckl, W. M.; Lackinger, M. *Chem. Commun.* **2011**, *47*, 12355.
(21) Faury, T.; Clair, S.; Abel, M.; Dumur, F.; Gigmes, D.; Porte, L. *J. Phys. Chem. C* **2012**, *116*, 4819.
(22) Dienstmaier, J. F.; Gigler, A. M.; Goetz, A. J.; Knochel, P.; Bein, T.; Lyapin, A.; Reichlmaier, S.; Heckl, W. M.; Lackinger, M. *ACS Nano* **2011**, *5*, 9737.
(23) Dienstmaier, J. F.; Medina, D. D.; Dogru, M.; Knochel, P.; Bein, T.; Heckl, W. M.; Lackinger, M. *ACS Nano* **2012**, *6*, 7234.
(24) Guan, C. -Z.; Wang, D.; Wan, L. -J. *Chem. Commun.* **2012**, *48*, 2943.
(25) Bieri, M.; Treier, M.; Cai, J.; Aït-Mansour, K.; Ruffieux, P.; Gröning, O.; Gröning, P.; Kastler, M.; Rieger, R.; Feng, X.; Müllen, K.; Fasel, R. *Chem. Commun.* **2009**, *45*, 6919.
(26) Weigelt, S.; Bombis, C.; Busse, C.; Knudsen, M. M.; Gothelf, K. V.; Lægsgaard, E.; Besenbacher, F.; Linderoth, T. R. *ACS Nano* **2008**, *2*, 651.
(27) Treier, M.; Fasel, R.; Champness, N. R.; Argent, S.; Richardson, N. V. *Phys. Chem. Chem. Phys.* **2009**, *11*, 1209.
(28) Coratger, R.; Calmettes, B.; Abel, M.; Porte, L. *Surf. Sci.* **2011**, *605*, 831.
(29) Méndez, J.; López, M. F.; Martín-Gago, J. A. *Chem. Soc. Rev.* **2011**, *40*, 4578.
(30) Lackinger, M.; Heckl, W. M. *J. Phys. D: Appl. Phys.* **2011**, *44*, 464011.
(31) Lafferentz, L.; Eberhardt, V.; Dri, C.; Africh, C.; Comelli, G.; Esch, F.; Hecht, S.; Grill, L. *Nat. Chem.* **2012**, *4*, 215.
(32) Champness, N. R. *Nat. Nanotechnol.* **2008**, *3*, 324.
(33) Gourdon, A. *Angew. Chem., Int. Ed.* **2008**, *47*, 6950.
(34) Perepichka, D. F.; Rosei, F. *Science* **2009**, *323*, 216.
(35) Anderson, S.; Anderson, H. L.; Sanders, J. K. M. *Acc. Chem. Res.* **1993**, *26*, 469.
(36) Diederich, F.; Stang, P. J. *Templated Organic Synthesis*, Wiley-VCH: Weinheim, Germany, 2000.
(37) Thompson, M. C.; Busch, D. H. *J. Am. Chem. Soc.* **1964**, *86*, 213.
(38) Sprafke, J. K.; Kondratuk, D. V.; Wykes, M.; Thompson, A. L.; Hoffmann, M.; Drevinskas, R.; Chen, W. -H.; Yong, C. K.; Kärnbratt, J.; Bullock, J. E.; Malfois, M.; Wasielewski, M. R.; Albinsson, B.; Herz, L. M.; Zigmantas, D.; Beljonne, D.; Anderson, H. L. *J. Am. Chem. Soc.* **2011**, *133*, 17262.
(39) Toh, N. L.; Nagarathinam, M.; Vittal, J. J. *Angew. Chem., Int. Ed.* **2005**, *117*, 2277.
(40) Hoffmann, S. *Angew. Chem., Int. Ed.* **1992**, *31*, 1013.
(41) Li, Y.; Lin, N. *Phys. Rev. B* **2011**, *84*, 125418.
(42) Adisoejoso, J.; Li, Y.; Liu, J.; Liu, P. N.; Lin, N. *J. Am. Chem. Soc.* **2012**, *134*, 18526.
(43) Heim, D.; Écija, D.; Seufert, K.; Auwärter, W.; Aurisicchio, C.; Fabbro, C.; Bonifazi, D.; Barth, J. V. *J. Am. Chem. Soc.* **2010**, *132*, 6783.
(44) Lafferentz, L.; Ample, F.; Yu, H.; Hecht, S.; Joachim, C.; Grill, L. *Science* **2009**, *323*, 1193.
(45) Wang, W.; Shi, X.; Wang, S.; Van Hove, M. A.; Lin, N. *J. Am. Chem. Soc.* **2011**, *133*, 13264.
(46) Nagahama, S.; Matsumoto, A. *J. Poly. Sci. A: Poly. Chem.* **2004**, *42*, 3922.